High-accuracy differential quadrature finite element method and its application to free vibrations of thin plate with curvilinear domain

Yufeng Xing*,† and Bo Liu

The Solid Mechanics Research Center, Beijing University of Aeronautics and Astronautics, Beijing 100191, China

SUMMARY

Based on the differential quadrature (DQ) rule, the Gauss Lobatto quadrature rule and the variational principle, a DQ finite element method (DQFEM) is proposed for the free vibration analysis of thin plates. The DQFEM is a highly accurate and rapidly converging approach, and is distinct from the differential quadrature element method (DQEM) and the quadrature element method (QEM) by employing the function values themselves in the trial function for the title problem.

The DQFEM, without using shape functions, essentially combines the high accuracy of the differential quadrature method (DQM) with the generality of the standard finite element formulation, and has superior accuracy to the standard FEM and FDM, and superior efficiency to the *p*-version FEM and QEM in calculating the stiffness and mass matrices.

By incorporating the reformulated DQ rules for general curvilinear quadrilaterals domains into the DQFEM, a curvilinear quadrilateral DQ finite plate element is also proposed. The inter-element compatibility conditions as well as multiple boundary conditions can be implemented, simply and conveniently as in FEM, through modifying the nodal parameters when required at boundary grid points using the DQ rules. Thus, the DQFEM is capable of constructing curvilinear quadrilateral elements with any degree of freedom and any order of inter-element compatibilities. A series of frequency comparisons of thin isotropic plates with irregular and regular planforms validate the performance of the DQFEM. Copyright © 2009 John Wiley & Sons, Ltd.

1. INTRODUCTION

The standard finite element method (FEM) and finite difference method (FDM) have been employed for the solution of a wide variety of engineering problems in the past. However, both FEM and

---

*Correspondence to: Yufeng Xing, The Solid Mechanics Research Center, Beijing University of Aeronautics and Astronautics, Beijing 100191, China.
†E-mail: xingyf@buaa.edu.cn

FDM typically use low-order schemes, and, consequently, high accuracy is achieved with some difficulties. In seeking alternative numerical algorithms, using less grid points with acceptably accurate solutions to differential equations, another numerical scheme called differential quadrature method (DQM) was introduced by Bellman et al. [1, 2]. The DQM has been experimented with and its general versatility has been established in a variety of physical problems, such as transport processes [3], structural mechanics [4–12], fluid mechanics [13–15] and some problems in chemical engineering [16, 17]. An exhaustive list of the literature on the DQM up to 1996 may be found in survey papers [18, 19]. The DQM was also referred to as the generalized collocation method in Reference [19]. Although the DQM as a numerically accurate and computationally efficient technique has been well demonstrated, its limitations summarized by Bert and Malik [18] are also apparent, which are reviewed below and given more comments incorporating the developments since then.

The DQM, by its very basis, is limited in application to the domains having boundaries that are aligned with the coordinate axes. But it is obvious that we can use the DQM to analyze irregular domains that are the assemblies of such regular domains using the domain decomposition ([20] for example) and the quadrature element ([21, 22] for example). Bert and Malik [5] have extended the DQM to curvilinear quadrilaterals by means of the natural-to-Cartesian geometric mapping technique, the quadrature rules were reformulated there. However, since the computational domain of the DQM is much larger than that of a finite element, the geometric mapping may cause significant errors when the domain is large and the boundary has a high curvature; hence, accurate transformation techniques are needed. The blending function method used by Malik and Bert [23] is such an approach, but higher-order serendipity mapping functions used by the authors in present study are another natural and general choice. Another work on irregular domains is that of Shu et al. [24] for the DQ solutions of the free vibration of thin plates with curvilinear boundaries. In their work, the exact geometric mapping using blending functions was utilized for transforming the governing equations from Cartesian to natural reference frame and the usual quadrature rules were then used for setting up the DQ analog equations, and much less computational effort and virtual storage were required.

The second limitation or problem, first pointed out by Civan and Sliepcevich [25], is the deterioration of the DQ solution with increasing number of grid points. This problem, basically, is how to space grid points. It has been well shown ([5, 7, 26, 27] for example) that the so-called Chebyshev–Gauss–Lobatto points, first used by Shu and Richards [14] and used widely since then, are better than the equally spaced, Legendre and Chebyshev points in a variety of problems.

Since the original DQM has only the function values at the grid points as independent variables, difficulty arises for applying multiple boundary conditions, for example, to solve fourth-order differential equations of beam or thin plate. To resolve this difficulty several different schemes have been investigated, see [28–31].

In δ-method [4, 6, 21], one boundary condition is exactly imposed while the other is approximately imposed only. Jang et al. [6] found that the δ-method was not equally successful for all structural problems with different boundary conditions if δ was not very small. Nevertheless, if δ is too small, the polynomial solution may oscillate.

The multiple boundary conditions can also be imposed by modifying weighting coefficient matrices [11, 12, 27, 28], in which the boundary conditions were built during the formulation of the weighting coefficients for higher-order derivative. However, Shu and Du [32, 33] reported that this technique had some major limitations and was not applicable to general boundary conditions, for example, free boundary conditions.

Another way to impose the boundary conditions is to apply the multiple boundary conditions at the same boundary points and to establish the DQ analogous equations of the boundary conditions at the boundary points. To eliminate the redundant equations, the DQ analogous equations of the governing differential equations at so-called auxiliary grid points are dropped. This approach has been used extensively by many researchers [8, 32–37] and was viewed as substituting all the boundary conditions into the governing equations [32].

Alternatively, the boundary conditions involving higher-order derivatives can be imposed exactly by modifying the trial functions to incorporate the degrees of freedom (DOFs) of the specified higher-order derivatives at the boundary [29, 30, 38–44]. In this approach, the first-order [44] and the second-order derivatives (see [29, 30] for example) were employed as the independent DOFs at boundary points, the Lagrange (see [43] for example) and Hermite (see [38, 42] for example) functions were commonly used in the determination of weighting coefficients. But in general, mixed-type boundary conditions cannot be tackled directly by this method. Additionally, Lu *et al.* [45] formulated the DQM in the state space, where the boundary conditions were dealt with without difficulties using state variables.

In a word, there are problems of feasibility, generality and simplicity in imposing the multiple boundary conditions (the free boundary condition of plates, for example), although several methods as aforementioned have been proposed.

All works via DQM yield good to excellent results due to the use of the high-order global basis functions in the computational domain. Nevertheless, further application of the method has been greatly restricted by its drawback of not being able to be directly employed to solve the problem with discontinuities [21]. To improve the versatility of the DQM, the DQ element method (DQEM) [26, 29, 30, 38, 41, 43, 44, 46–49] was formulated from the strong forms of the governing equations. The trial functions include the slopes or curvatures for implementing multiple boundary conditions, in this sense the method differs from the original idea of the DQM wherein only the function values are used in trial functions.

As is well known, the FEM is famous for its versatility and its simplicity in imposing the inter-element compatibility conditions and boundary conditions. Using the *p*-version element with higher-order polynomials, an entire plate can be modeled by one such element without loss of accuracy. For example, the convergence of the 49-DOF rectangular quadrature plate element [50, 51] is more rapid than that of the *h*-version elements using the same number of DOFs. However, it is not easy to formulate the shape functions in the *p*-version FEM and the QEM with higher-order polynomials. Once the DOFs change, the shape functions must be recalculated. Therefore, the *p*-version FEM and the QEM [50, 51] lack adaptability, the calculation of the stiffness and mass matrices is expensive and the cost will increase dramatically when using curvilinear quadrilateral elements. Moreover, one would encounter difficulties in formulating complete compatible thin plate element due to the requirements of C^1 continuity, thus commonly used quadrilateral element of thin plate has 12 DOFs, and is a partial compatible plate element.

In present study the DQ rules in conjunction with the Gauss–Lobatto quadrature rules are used to discretize the energy functional that is generally used to derive the FEM formulation. This novel method is called the DQ finite element method (DQFEM), where the boundary conditions can be simply imposed as in FEM, the shape functions are not needed any more and the stiffness and mass matrices can be obtained by simple algebraic operations of the weighting coefficient matrices of the DQ rules and Gauss–Lobatto quadrature rule. Consequently, the efficiency is improved dramatically while the high accuracy of the DQM is maintained. The inter-element compatibility conditions are implemented through modifying the nodal displacement vector using the DQ rules.

The advantages of the DQFEM can be briefly summarized as follows: (1) there are not slopes or curvatures in trial functions, i.e. the Lagrange polynomials are used as trial function even though for thin plate, this is consistent to the original idea of the DQM. (2) The slopes or/and curvatures can be involved at boundary grid points when required for imposing multiple boundary conditions via the transformation of nodal displacement vector using DQ rules. (3) The node shape functions are not necessary, the stiffness and mass matrices can be computed by simple multiplications of the weighting coefficient matrices of the DQ rules and Gauss–Lobatto quadrature rule. (4) The assemblage of elements and implementation of boundary conditions are exactly the same as in the standard FEM.

The title problem or the free vibrations of isotropic thin plates with different planforms have been studied extensively due to a variety of applications by using the FEM [52–56], the Ritz method [57–63], the DQM [5, 23, 64–70], the discrete singular convolution (DSC) method [71–73], the superposition method [74–76], the Green function method [77], the moving least-square Ritz method [78] and the Galerkin method [79]. In the above paragraph there are some comments on FEM and DQM. The Ritz method featured by high accuracy, easy coding and capabilities of accommodating a wide spectrum of plate configurations and boundary constraints is computationally expensive and cannot be used to solve problems with complex geometry and discontinuities. The DSC method, with formula similar to the DQM, is a localized method and numerically more stable than the DQM for problems requiring a large number of grid points [80]. However, the applications of the DSC method to vibrations of plates are limited in straight-sided quadrilateral plates so far. It is noteworthy, recently, that some new exact solutions have been obtained by the present authors using direct separation of variables for rectangular plates with any combinations of simple support and clamp conditions [81, 82].

In this context, by incorporating the reformulated DQ rules into the DQFEM, the curvilinear quadrilateral DQ finite element is also formulated in this paper. Therefore, the DQFEM is capable of constructing curvilinear quadrilateral elements with any DOF and any order of inter-element continuity. The performance of the DQFEM is demonstrated through free vibration analysis of thin isotropic plates with sectorial, circular, triangular, pentagonal, trapezoidal and rhombic planforms. In all numerical tests, the DQFEM results are found to be convergent, and in excellent agreement with results in literature and of the FEM.

The outline of this paper is as follows. The DQ rule and Gauss–Lobatto quadrature rule are reviewed briefly in Sections 2 and 3, respectively. The formulation of DQFEM is presented in Section 4 where the QEM [50, 51] is also reviewed. In Section 5, the numerical results are compared with available results. Finally, the conclusions are drawn.

2. THE DQ RULE

Details of the DQM can be found in literature, for example, the survey paper [18]. Only the two-dimensional DQ rules used in the present study are given in a compact form as follows. The rth-order, the sth-order and the $(r+s)$th-order partial derivatives of $f(x, y)$ at point (x_i, y_j) can be expressed as:

$$\left.\frac{\partial^r f}{\partial x^r}\right|_{ij} = \sum_{m=1}^{M} A_{im}^{(r)} f_{mj}, \quad \left.\frac{\partial^s f}{\partial y^s}\right|_{ij} = \sum_{n=1}^{N} B_{jn}^{(s)} f_{in}, \quad \left.\frac{\partial^{r+s} f}{\partial x^r \partial y^s}\right|_{ij} = \sum_{m=1}^{M} A_{im}^{(r)} \sum_{n=1}^{N} B_{jn}^{(s)} f_{mn} \qquad (1)$$

The direct application of the DQ rules in Equation (1) is cumbersome. Here, they are written in a compact form using a single index notation for grid points by defining the following vector and matrices:

$$\bar{\mathbf{f}} = [f_{11} \ \ldots \ f_{M1} \ f_{12} \ \ldots \ f_{M2} \ \ldots \ f_{1N} \ \ldots \ f_{MN}]^{\mathrm{T}} \tag{2}$$

$$\bar{\mathbf{A}}^{(r)} = \begin{bmatrix} \mathbf{A}^{(r)} & \mathbf{O} & \ldots & \mathbf{O} \\ \mathbf{O} & \mathbf{A}^{(r)} & \ldots & \mathbf{O} \\ \vdots & \vdots & \ddots & \vdots \\ \mathbf{O} & \mathbf{O} & \ldots & \mathbf{A}^{(r)} \end{bmatrix}, \quad \bar{\mathbf{B}}^{(s)} = \begin{bmatrix} \mathbf{B}_{11}^{(s)} & \mathbf{B}_{12}^{(s)} & \ldots & \mathbf{B}_{1N}^{(s)} \\ \mathbf{B}_{21}^{(s)} & \mathbf{B}_{22}^{(s)} & \ldots & \mathbf{B}_{2N}^{(s)} \\ \vdots & \vdots & \ddots & \vdots \\ \mathbf{B}_{N1}^{(s)} & \mathbf{B}_{N2}^{(s)} & \ldots & \mathbf{B}_{NN}^{(s)} \end{bmatrix} \tag{3}$$

where $\bar{\mathbf{A}}^{(r)}$ and $\bar{\mathbf{B}}^{(s)}$ are $(M \times N) \times (M \times N)$ matrices, $\mathbf{B}_{ij}^{(s)} = \mathrm{diag}(B_{ij}^{(s)}, \ldots, B_{ij}^{(s)})_{M \times M}$ and $\mathbf{A}^{(r)} = (A_{ij}^{(r)})_{M \times M}$. Thus, Equation (1) becomes

$$\left. \frac{\partial^r f}{\partial x^r} \right|_k = \sum_{m=1}^{M \times N} \bar{A}_{km}^{(r)} \bar{f}_m, \quad \left. \frac{\partial^s f}{\partial y^s} \right|_k = \sum_{m=1}^{M \times N} \bar{B}_{km}^{(s)} \bar{f}_m, \quad \left. \frac{\partial^{r+s} f}{\partial x^r \partial y^s} \right|_k = \sum_{m=1}^{M \times N} \bar{F}_{km}^{(r+s)} \bar{f}_m \tag{4}$$

where $k, m = (j-1)M + i$, $(i = 1, 2, \ldots, M; j = 1, 2, \ldots, N)$. It is noteworthy that the two matrices defined by Equation (3) can also be obtained by the standard tensor product as

$$\bar{\mathbf{A}}^{(r)} = \mathbf{E} \otimes \mathbf{A}^{(r)} \tag{5a}$$

$$\bar{\mathbf{B}}^{(s)} = \mathbf{B}^{(s)} \otimes \mathbf{E} \tag{5b}$$

where $\mathbf{B}^{(s)} = (B_{ij}^{(s)})_{N \times N}$, $\mathbf{E}$ is an $N \times N$ unit matrix for Equation (5a) and an $M \times M$ unit matrix for Equation (5b). Denote $\bar{\mathbf{F}}^{(r+s)} = \bar{\mathbf{A}}^{(r)} \bar{\mathbf{B}}^{(s)}$, we have

$$\bar{\mathbf{F}}^{(r+s)} = \bar{\mathbf{A}}^{(r)} \bar{\mathbf{B}}^{(s)} = \bar{\mathbf{B}}^{(s)} \bar{\mathbf{A}}^{(r)} = \mathbf{B}^{(s)} \otimes \mathbf{A}^{(r)} \tag{6}$$

The correctness of Equation (6) can be readily verified by substituting Equation (5) into Equation (6) and using the theorem $(\mathbf{A} \otimes \mathbf{B})(\mathbf{C} \otimes \mathbf{D}) = \mathbf{AC} \otimes \mathbf{BD}$, where $\mathbf{A}$, $\mathbf{B}$, $\mathbf{C}$ and $\mathbf{D}$ are four generic matrices with compatible dimensions. $\bar{\mathbf{F}}^{(r+s)}$, $\bar{\mathbf{A}}^{(r)}$ and $\bar{\mathbf{B}}^{(s)}$ are used in Section 4.

3. GAUSS–LOBATTO QUADRATURE RULE

The well-known Gauss–Lobatto quadrature available in most mathematics handbooks is the Gauss integration with two endpoints fixed, but it is briefly introduced here to make the paper self-contained. The Gauss–Lobatto quadrature rule with precision degree $(2n-3)$ for function $f(x)$ defined within $[-1, 1]$ is

$$\int_{-1}^{1} f(x) \, \mathrm{d}x = \sum_{j=1}^{n} C_j f(x_j) \tag{7}$$

where the weights C_j are given by

$$C_1 = C_n = \frac{2}{n(n-1)}, \quad C_j = \frac{2}{n(n-1)[P_{n-1}(x_j)]^2} \quad (j \neq 1, n) \tag{8}$$

where x_j is the $(j-1)$th zero of $P'_{n-1}(x)$, and the Legendre polynomial $P_n(x)$ of degree n has the form

$$P_n(x) = \sum_{k=0}^{[n/2]} \frac{(-1)^k (2n-2k)!}{2^n k!(n-k)!(n-2k)!} x^{n-2k} \tag{9}$$

The zeros of $P'_{n-1}(x)$ are the same as the eigenvalues of its companion matrix. The companion matrix of a polynomial $c_1 x^n + c_2 x^{n-1} + \cdots + c_n x + c_{n+1}$ is

$$B = \begin{bmatrix} b_1 & b_2 & \dots & b_{n-1} & b_n \\ 1 & 0 & \dots & 0 & 0 \\ 0 & 1 & \dots & 0 & 0 \\ \vdots & \vdots & \ddots & \vdots & \vdots \\ 0 & 0 & \dots & 1 & 0 \end{bmatrix} \tag{10}$$

where $b_j = -c_{j+1}/c_1 (j = 1, 2, \ldots, n)$.

4. FORMULATION OF THE DQFEM PLATE ELEMENT

4.1. The quadrature element method (QEM)

In general, the convergence of the p-version elements is more rapid than that of the h-version elements in a finite element analysis using the same number of DOFs. One whole plate can be modeled by just one p-version element satisfying the accuracy requirement. In the following, the quadrature plate element [50, 51], a 25-node rectangular element with 49 DOFs as shown in Figure 1, is recalled. The displacement field of the 49-DOFs quadrature plate element is expressed in terms of polynomial-type shape functions such that the displacement of the element is assumed as

$$w(x, y) = \sum_{i=1,2,3,4} [N_{i1}w_i + N_{i2}w_{ix} + N_{i3}w_{iy} + N_{i4}w_{ixy}] + \sum_{i=17-25} [N_{i1}w_i]$$

$$+ \sum_{i=5,6,7,11,12,13} [N_{i1}w_i + N_{i2}w_{ix}] + \sum_{i=8,9,10,14,15,16} [N_{i1}w_i + N_{i2}w_{iy}] \tag{11}$$

where w_i, $w_{ix} = (\partial w/\partial x)_i$, $w_{iy} = (\partial w/\partial y)_i$ and $w_{ixy} = (\partial^2 w/\partial x \partial y)_i$ are the local DOFs of node i. Then one can obtain the ordinary dynamic equations of thin plate by substituting the displacement
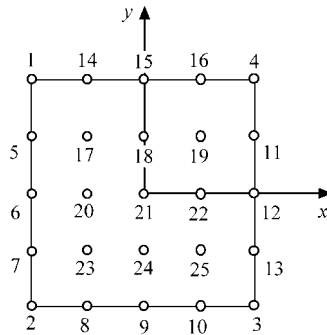
Figure 1. The nodal configuration of a quadrature plate element.

function into the strain energy U and the work potential W and using the variational principle $\delta(U+W)=0$. For thin plate, U and W have the forms as

$$U = \frac{D}{2} \iint_S \left[\left(\frac{\partial^2 w}{\partial x^2}\right)^2 + \left(\frac{\partial^2 w}{\partial y^2}\right)^2 + 2v\frac{\partial^2 w}{\partial x^2}\frac{\partial^2 w}{\partial y^2} + 2(1-v)\left(\frac{\partial^2 w}{\partial x \partial y}\right)^2 \right] dx\, dy \qquad (12)$$

$$W = -\iint_S w\left(-\rho h\frac{\partial^2 w}{\partial t^2}\right) dx\, dy - \iint_S wq\, dx\, dy \qquad (13)$$

Using the above QEM, quite accurate results were obtained [50, 51] with relative small number of DOFs. It is notable that the QEM based on the trial function (11) is analogous to DQM due to using deflections themselves at inner grid points, and to FEM due to using nodal shape functions and slopes in trial functions as well as variational principle.

4.2. The DQ finite element method

To improve the computational efficiency and simplify the implementation of boundary conditions of the QEM while maintaining its high accuracy motivate the development of a new method, referred to as the DQ finite element method (DQFEM) in the present study. In this novel method, the Lagrange polynomials are chosen as the trial function of C^1 thin plate element as

$$w(x, y) = \sum_{i=1}^{M} \sum_{j=1}^{N} l_i(x)l_j(y)w_{ij} \qquad (14)$$

It should be emphasized that there are no slopes and curvatures in expression (14), which differs from the trial functions used in FEM, QEM and DQEM for thin plate.

Substituting the trial function into Equations (12) and (13) and using the DQ rules in conjunction with the Gauss–Lobatto quadrature rule, one can have

$$U = \frac{D}{2} \sum_{k=1}^{K} C_k \{ [\bar{\mathbf{A}}_k^{(2)}\bar{\mathbf{w}}]^2 + [\bar{\mathbf{B}}_k^{(2)}\bar{\mathbf{w}}]^2 + 2v[\bar{\mathbf{A}}_k^{(2)}\bar{\mathbf{w}}][\bar{\mathbf{B}}_k^{(2)}\bar{\mathbf{w}}] + 2(1-v)[\bar{\mathbf{F}}_k^{(1+1)}\bar{\mathbf{w}}]^2 \} \qquad (15)$$

$$W = \sum_{k=1}^{K} C_k \left[w_k \left(\rho h \frac{\partial^2 w_k}{\partial t^2} \right) - w_k q_k \right] \tag{16}$$

where $K = M \times N$, $C_k = C_i^x C_j^y$, $\bar{\mathbf{A}}_k^{(2)}$, $\bar{\mathbf{B}}_k^{(2)}$ and $\bar{\mathbf{F}}_k^{(1+1)}$ are the kth rows of $\bar{\mathbf{A}}^{(2)}$, $\bar{\mathbf{B}}^{(2)}$ and $\bar{\mathbf{F}}^{(1+1)}$, respectively. $\bar{\mathbf{w}} = (w_m)_{K \times 1}$ is a column vector, here $m = (j-1)M + i$, $i = 1, \dots, M$, $j = 1, \dots, N$. For brevity, let $\mathbf{A} = \bar{\mathbf{A}}^{(2)}$, $\mathbf{B} = \bar{\mathbf{B}}^{(2)}$, $\mathbf{F} = \bar{\mathbf{F}}^{(1+1)}$, $\mathbf{C} = \text{diag}[C_k]$, then Equations (15) and (16) can be rewritten as

$$U = \frac{D}{2} \bar{\mathbf{w}}^{\mathrm{T}} [\mathbf{A}^{\mathrm{T}} \mathbf{C} \mathbf{A} + \mathbf{B}^{\mathrm{T}} \mathbf{C} \mathbf{B} + 2 \upsilon \mathbf{A}^{\mathrm{T}} \mathbf{C} \mathbf{B} + 2(1 - \upsilon) \mathbf{F}^{\mathrm{T}} \mathbf{C} \mathbf{F}] \bar{\mathbf{w}} \tag{17}$$

$$W = \bar{\mathbf{w}}^{\mathrm{T}} (\rho h \mathbf{C}) \ddot{\bar{\mathbf{w}}} + \bar{\mathbf{w}}^{\mathrm{T}} \mathbf{C} \mathbf{q} \tag{18}$$

For imposing the inter-element compatibility conditions of any order, some modification on the displacement vector $\bar{\mathbf{w}}$ is necessary. One choice of the displacement vectors satisfying the C^1 inter-element compatibility conditions for rectangular thin plate element, as shown in Figure 2, can be given by

$$\mathbf{w} = [w_m \ w_{mx} \ w_{my} \ w_{mxy} \ (i=1, M; j=1, N), \ w_m \ w_{mx} \ (i=3, \dots, M-2; j=1, N)$$

$$w_m \ w_{my} \ (i=1, M; j=3, \dots, N-2), \ w_m \ (i=3, \dots, M-2; j=3, \dots, N-2)] \tag{19}$$

which is similar to nodal parameters used in trial function (11). For a curvilinear quadrilateral element as shown in Figure 3, the derivatives of w in Equation (19) should be defined with respect to the normal and tangential of the edge. The vector $\bar{\mathbf{w}}$ is related to $\mathbf{w}$ by the DQ rules, as

$$\mathbf{w} = \mathbf{Q} \bar{\mathbf{w}} \tag{20}$$

where $\mathbf{Q}$ is not singular for any case, and a diagonal unit matrix for C^0 element, this cause mass matrix given below to be a diagonal matrix, see Equation (22). Substitution of Equation (20) into Equations (17) and (18) yields the stiffness matrix, the mass matrix and the force vector of the new rectangular thin plate, as

$$\mathbf{K} = D \mathbf{Q}^{-\mathrm{T}} [\mathbf{A}^{\mathrm{T}} \mathbf{C} \mathbf{A} + \mathbf{B}^{\mathrm{T}} \mathbf{C} \mathbf{B} + \upsilon (\mathbf{A}^{\mathrm{T}} \mathbf{C} \mathbf{B} + \mathbf{B}^{\mathrm{T}} \mathbf{C} \mathbf{A}) + 2(1 - \upsilon) \mathbf{F}^{\mathrm{T}} \mathbf{C} \mathbf{F}] \mathbf{Q}^{-1} \tag{21}$$

$$\mathbf{M} = \mathbf{Q}^{-\mathrm{T}} (\rho h \mathbf{C}) \mathbf{Q}^{-1}, \quad \mathbf{R} = \mathbf{Q}^{-\mathrm{T}} (\mathbf{C} \mathbf{q}) \tag{22}$$

Apparently, both $\mathbf{K}$ and $\mathbf{M}$ are symmetrical matrices implying good numerical properties, but, generally, they are unsymmetrical in DQEM. Moreover, the above formulations for DQFEM are simpler and more adaptable, and hold for plates with irregular shape as shown below.

4.3. Curvilinear quadrilateral plate element

Since the DQ rules cannot be used directly for irregular domain, the reformulated DQ rules proposed by Bert and Malik [5] are employed in the present study. For completeness, reformulated DQ rules are recurred below, but it is worth mentioning that they were used to discretize the differential equation in Reference [5], where convergence problems were encountered when there are high-order derivatives on the boundary, while they are used to discretize the functional U and W here and the aforementioned convergence problems are avoided.
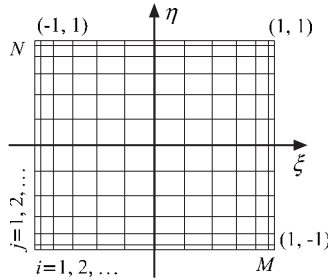
Figure 2. A square parent region.
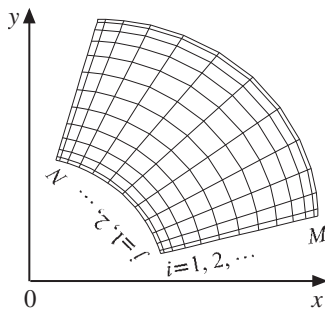
Figure 3. A sectorial region.

Let the interested domain be a curvilinear quadrilateral in the Cartesian x–y plane, as shown in Figure 4(a). The geometric mapping of this domain can be accomplished from a square parent domain, $-1 < \xi < 1$, $-1 < \eta < 1$ in the natural ξ–η plane, as shown in Figure 4(b), by using the coordinate transformation

$$x = \sum_{k=1}^{N_s} S_k(\xi, \eta) x_k, \quad y = \sum_{k=1}^{N_s} S_k(\xi, \eta) y_k \tag{23}$$

where x_k, y_k; $k = 1, 2, \ldots, N_s$ are the coordinates of N_s grid points on the boundaries of the domain. Since S_k has a unity value at the kth node and zeros at the remaining $(N_s - 1)$ nodes, the domain mapped by Equation (23) matches with the given quadrilateral domain exactly at the nodes on the boundaries.

Subsequently, we should express the derivatives of a function $f(x, y)$ with respect to x and y coordinates in terms of its derivatives with respect to ξ and η coordinates. Regarding $f(x, y)$ as an implicit function of ξ and η as $f = f[x(\xi, \eta), y(\xi, \eta)]$, and using the chain rule of differentiation, we have the following results:

$$\frac{\partial f}{\partial x} = \frac{1}{|\mathbf{J}|}\left(\frac{\partial y}{\partial \eta}\frac{\partial f}{\partial \xi} - \frac{\partial y}{\partial \xi}\frac{\partial f}{\partial \eta}\right), \quad \frac{\partial f}{\partial y} = \frac{1}{|\mathbf{J}|}\left(\frac{\partial x}{\partial \xi}\frac{\partial f}{\partial \eta} - \frac{\partial x}{\partial \eta}\frac{\partial f}{\partial \xi}\right) \tag{24}$$

Figure 4. (a) A curvilinear quadrilateral region in Cartesian x-y plane and (b) a square parent domain in natural ξ–η plane.
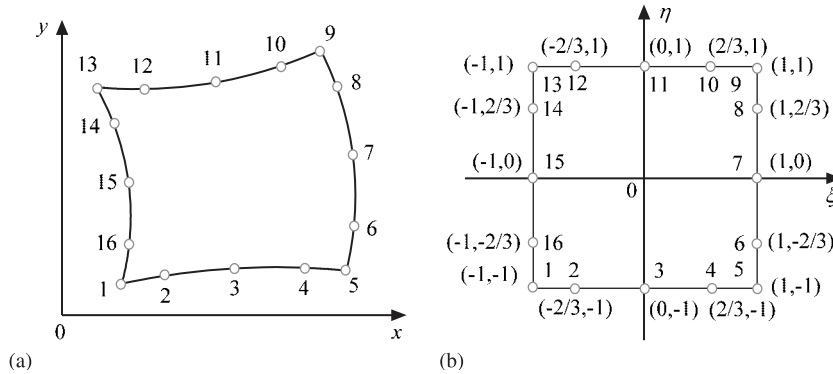
where the determinant $|\mathbf{J}|$ of $\mathbf{J} = \partial(x, y)/\partial(\xi, \eta)$ is

$$|\mathbf{J}| = \frac{\partial x}{\partial \xi}\frac{\partial y}{\partial \eta} - \frac{\partial y}{\partial \xi}\frac{\partial x}{\partial \eta} \qquad (25)$$

Since the parent domain is regular, the partial derivatives of function f with respect to the natural coordinates (ξ, η) at the pre-specified gird points can be obtained directly through the DQ rules. Consider the parent domain with $M \times N$ grid points, as shown in Figure 2. The first-order derivatives $\partial f/\partial \xi$ and $\partial f/\partial \eta$ at grid point (ξ_i, η_j) can be obtained by the DQ rules

$$\left.\frac{\partial f}{\partial \xi}\right|_{ij} = \sum_{m=1}^{M} A_{im}^{(1)} f_{mj}, \qquad \left.\frac{\partial f}{\partial \eta}\right|_{ij} = \sum_{n=1}^{N} B_{jn}^{(1)} f_{in} \qquad (26)$$

where $f_{ij} = f(\xi_i, \eta_j)$, $A_{im}^{(1)}$ are the first-order ξ-derivative weighting coefficients associated with the point $\xi = \xi_i$, $B_{jn}^{(1)}$ the first-order η-derivative weighting coefficients associated with the point $\eta = \eta_j$. Then the partial derivatives $\partial f/\partial x$ and $\partial f/\partial y$ at the gird point $x_{ij} = x(\xi_i, \eta_j)$, $y_{ij} = y(\xi_i, \eta_j)$ in the mapped curvilinear quadrilateral domain, as shown in Figure 3, can be computed by inserting Equation (26) into Equation (24), as

$$\left(\frac{\partial f}{\partial x}\right)_{ij} = \frac{1}{|\mathbf{J}|_{ij}}\left[\left(\frac{\partial y}{\partial \eta}\right)_{ij}\left(\sum_{m=1}^{M} A_{im}^{(1)} f_{mj}\right) - \left(\frac{\partial y}{\partial \xi}\right)_{ij}\left(\sum_{n=1}^{N} B_{jn}^{(1)} f_{in}\right)\right] \qquad (27)$$

$$\left(\frac{\partial f}{\partial y}\right)_{ij} = \frac{1}{|\mathbf{J}|_{ij}}\left[\left(\frac{\partial x}{\partial \xi}\right)_{ij}\left(\sum_{n=1}^{N} B_{jn}^{(1)} f_{in}\right) - \left(\frac{\partial x}{\partial \eta}\right)_{ij}\left(\sum_{m=1}^{M} A_{im}^{(1)} f_{mj}\right)\right] \qquad (28)$$

where the subscript ij refers to grid point (ξ_i, η_j) and its mapped point (x_{ij}, y_{ij}). Equations (27) and (28) define the DQ rules of the first order partial derivatives with respect to x and y coordinates

for the irregular domain. Certainly, the reformulated DQ rules can also be written in a compact form using a single index for grid points, as

$$\left.\frac{\partial f}{\partial x}\right|_k = \sum_{m=1}^{M \times N} \tilde{A}_{km}^{(1)} \bar{f}_m, \qquad \left.\frac{\partial f}{\partial y}\right|_k = \sum_{m=1}^{M \times N} \tilde{B}_{km}^{(1)} \bar{f}_m \qquad (29)$$

for $k, m = (j-1)M + i$; $i = 1, 2, \ldots, M$; $j = 1, 2, \ldots, N$. Thus, the transformation is fulfilled with an additional relation as follows:

$$dx\, dy = |\mathbf{J}|\, d\xi\, d\eta \qquad (30)$$

its proof may be found in calculus books, and is not repeated here. In the similar way as in Equation (3), we can formulated the matrices $\tilde{\mathbf{A}}^{(2)}$, $\tilde{\mathbf{B}}^{(2)}$. Let $\mathbf{A} = \tilde{\mathbf{A}}^{(2)}$, $\mathbf{B} = \tilde{\mathbf{B}}^{(2)}$, $\mathbf{F} = \tilde{\mathbf{A}}^{(1)}\tilde{\mathbf{B}}^{(1)}$, $\mathbf{C} = \mathrm{diag}[C_k J_k]$, where $J_k = |\mathbf{J}|_{ij}$, then the stiffness matrix $\mathbf{K}$, mass matrix $\mathbf{M}$ and load vector $\mathbf{R}$ for curvilinear quadrilateral plate element can be determined by substituting $\mathbf{A}$, $\mathbf{B}$, $\mathbf{C}$ and $\mathbf{F}$ into Equations (21) and (22).

5. NUMERICAL COMPARISONS

This section aims to demonstrate the high accuracy and rapid convergence of the DQFEM through free vibration analysis of thin isotropic plates with sectorial (Figure 5), elliptical (Figure 6), triangular (Figure 7), pentagonal (Figure 8), trapezoidal (Figure 9) and rhombic (Figure 10) planforms. The triangular and pentagonal plates are divided into three sub quadrilateral plates in the analysis, as shown in Figures 7 and 8. The mappings of a square parent domain to the interested domains are carried out via the quartic or cubic serendipity interpolation functions. Each table of the frequencies includes the formula for Ω. Many available exact and numerical results in literature are used for comparisons where the Poisson ratio is 0.3, the numbers of grid points $N = M$ for numerical convenience.

The frequencies are presented in Tables I–VIII, where various boundary conditions are taken into account for a range of the grid points to show numerically the convergence behavior of DQFEM, to five or six significant digits in order to show the convergence rate more evidently.

In Table I the results are for two types of sectorial plates, namely, a plate with four simply supported (S) edges ($SSSS$), and a plate with two simply supported radial edges and two clamped (C)
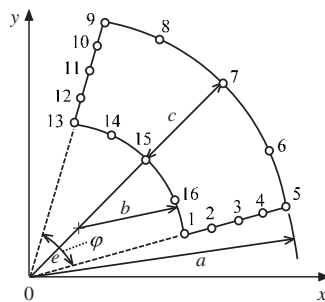
Figure 5. An eccentric sectorial plate.
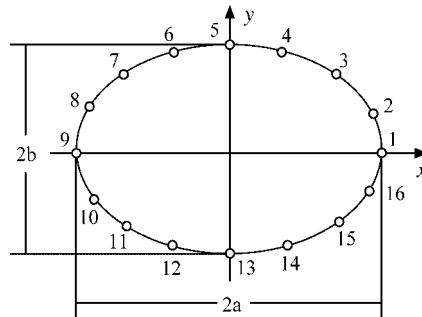
Figure 6. An elliptic plate.
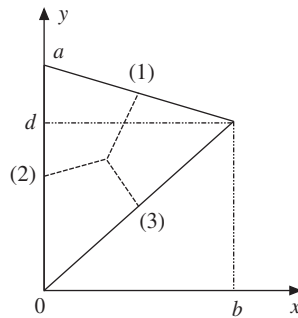
Figure 7. A triangular plate.
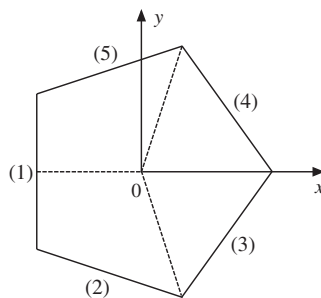
Figure 8. A pentagonal plate.

circumferential edges (*SCSC*). Table I also includes the exact results [83] using the methodology of Ramakrishnan and Kunukkaserll [84], the Rayleigh–Ritz solutions [83] using eight-term orthogonal polynomials and the DQM results [23] using both cubic serendipity interpolation functions and blending functions. It is shown that all numerical results except for the ones obtained through cubic serendipity functions agree well with the exact results, mostly to five significant digits. The
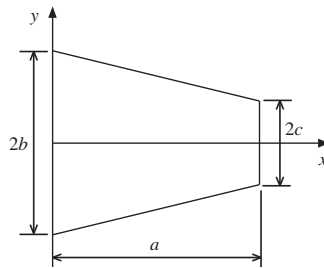
Figure 9. A symmetric trapezoidal plate.
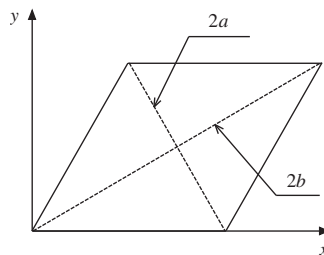
Figure 10. A rhombic plate.

cubic serendipity interpolations exhibit some convergence and accuracy problems [23]. Apparently, both quartic and cubic serendipity functions embedded in the DQFEM exhibit better convergence than the blending-function and the cubic serendipity function in the DQM. Moreover, the DQFEM results with the quartic interpolation functions and the DQM results with the blending functions are closer to the exact results.

In Tables II and III, a sectorial plate with two eccentric circular arcs, and an elliptical plate with ellipticities $a/b=1$ and 2 are investigated, respectively. Their planforms are more irregular than that considered in Table I.

The eccentric sectorial plates in Table II have simple support, clamp and free edges, and at least a straight edge is free. The DQFEM frequencies are compared only with the FEM results computed by the authors using MSC/NASTRAN due to the lack of published results. In Bert and Malik's reformulated DQM formulation [5], the convergence of the solution for plates with free edges was found to be severely slow, but the DQFEM solutions show excellent convergences for the four cases with at least a free edge, this may attribute to the same imposing method of free boundary conditions and symmetrical matrices in DQFEM as in FEM.

The DQFEM solutions for the clamped circular ($a/b=1$) and elliptic ($a/b=2$) plates are compared, in Table III, with the exact solutions [85], the reformulated DQM solutions [5], and the Rayleigh–Ritz solutions [86, 87] using orthogonal polynomials. It can be seen that the DQFEM frequencies agree with the exact and Rayleigh–Ritz results, mostly to four significant digits, but the reformulated DQM solutions do not show any convergence with the increase of grid points due to the lower-order mapping function and unsymmetrical stiffness and mass matrices used there.

Table I. The first four natural frequencies of sectorial plates
(a/b=2.0, e/b=0.0, φ=45^0, $\Omega=\omega a^2\sqrt{\rho h/D}$).

| | Mode sequences | | | | | | | |
| | 1 | 2 | 3 | 4 | 1 | 2 | 3 | 4 |
$M=N$	SSSS plate				SCSC plate			
Exact solutions [83]								
—	68.379	150.98	189.60	278.39	107.57	178.82	269.49	305.84
Eight-term orthogonal-polynomial Rayleigh-Ritz solutions [83]								
—	68.379	150.98	189.60	278.39	107.57	178.82	269.49	305.84
DQFEM solutions with quartic serendipity interpolation functions								
8	68.374	150.97	189.54	281.67	107.57	178.84	269.53	309.32
9	68.378	150.98	189.59	278.37	107.57	178.82	269.57	305.85
10	68.379	150.98	189.59	278.43	107.57	178.82	269.49	305.89
11	68.379	150.98	189.60	278.38	107.57	178.82	269.49	305.84
12	68.379	150.98	189.60	278.39	107.57	178.82	269.49	305.84
13	68.379	150.98	189.60	278.39	107.57	178.82	269.49	305.84
DQM solutions with blending functions [23]								
11	68.379	150.98	189.60	278.17	107.57	178.82	269.51	305.63
12	68.379	150.98	189.60	278.42	107.57	178.82	269.49	305.88
13	68.379	150.98	189.60	278.38	107.57	178.82	269.49	305.84
14	68.379	150.98	189.60	278.39	107.57	178.82	269.49	305.84
15	68.379	150.98	189.60	278.39	107.57	178.82	269.49	305.84
DQFEM solutions with cubic serendipity interpolation functions								
8	68.375	150.94	189.54	281.61	107.58	178.81	269.53	309.26
9	68.379	150.95	189.59	278.33	107.57	178.79	269.58	305.81
10	68.380	150.95	189.59	278.38	107.57	178.79	269.50	305.85
11	68.381	150.95	189.60	278.34	107.57	178.79	269.50	305.80
12	68.381	150.95	189.60	278.34	107.57	178.79	269.50	305.80
DQM solutions with cubic serendipity interpolation functions [23]								
11	68.364	150.94	189.62	279.31	107.57	178.79	269.52	305.58
12	68.378	150.91	189.57	278.38	107.57	178.79	269.49	305.84
13	68.376	150.95	189.60	278.12	107.57	178.79	269.50	305.80
14	68.379	150.95	189.60	278.34	107.57	178.79	269.50	305.80
15	68.378	150.95	189.60	278.35	107.57	178.79	269.50	305.80

In Table IV, comparison studies are carried out for rectangular plates with four combinations of simply supported, clamped and free edges. It is shown that DQFEM solutions agree very closely with the Kantorovich solutions [88] for *CSCS* and *FSFS* plates, with the double trigonometric series solution [89] for *CCCC* plate, even to all available significant digits, and with FEM results for *FFFF* plate to four significant digits, this implies that the DQFEM precision is independent of boundary conditions.

Table V presents comparison studies of five triangular plates with five combinations of simply supported, clamped and free edges, and one corner-supported triangular plate. *CSS* indicates that the side (1), side (2) and side (3) of the triangle are clamped, simply supported and simply supported, respectively, and so forth. DQFEM solutions are in excellent agreement, at least to three significant digits, with the Rayleigh–Ritz solutions [62] and the superposition solutions [75]. The same

Table II. The first four natural frequencies for eccentric sectorial plates
$(a/b=\frac{8}{3},\ e/b=1.0,\ \varphi=45^0,\ \Omega=\omega(a^2/\pi^2)\sqrt{\rho h/D})$.

	Mode sequences
	1	2	3	4	1	2	3	4
$M=N$	\multicolumn{4}{c	}{FSSS plate}	\multicolumn{4}{c	}{FSCS plate}
Finite element analysis solutions								
—	13.356	18.819	26.157	37.837	13.368	19.694	27.980	40.696
DQFEM solutions with quartic serendipity interpolation functions								
8	13.359	18.821	26.165	38.528	13.371	19.700	28.003	42.212
9	13.358	18.819	26.165	37.857	13.369	19.696	27.989	40.717
10	13.357	18.819	26.163	37.856	13.369	19.695	27.986	40.736
11	13.357	18.819	26.162	37.842	13.369	19.695	27.985	40.700
12	13.357	18.819	26.162	37.842	13.369	19.695	27.985	40.700
DQFEM solutions with cubic serendipity interpolation functions								
8	13.415	18.805	26.178	38.508	13.428	19.669	28.016	42.164
9	13.414	18.804	26.176	37.867	13.426	19.666	27.994	40.723
10	13.413	18.804	26.175	37.860	13.425	19.664	27.993	40.732
11	13.413	18.804	26.174	37.849	13.425	19.664	27.992	40.701
12	13.413	18.804	26.174	37.848	13.425	19.664	27.992	40.700
13	13.413	18.804	26.174	37.848	13.425	19.664	27.992	40.700
	\multicolumn{4}{c	}{FSFS plate}	\multicolumn{4}{c	}{FFFF plate}
Finite element analysis solutions								
—	13.087	13.708	20.863	29.507	4.6382	6.7017	12.559	15.530
DQFEM solutions with quartic serendipity interpolation functions								
8	13.090	13.712	20.877	29.521	4.6389	6.7042	12.569	15.561
9	13.087	13.712	20.868	29.522	4.6381	6.7041	12.569	15.534
10	13.087	13.711	20.867	29.514	4.6381	6.7040	12.558	15.535
11	13.087	13.711	20.867	29.514	4.6381	6.7040	12.558	15.534
12	13.087	13.710	20.867	29.514	4.6381	6.7040	12.558	15.534
13	13.087	13.710	20.867	29.514	4.6381	6.7040	12.558	15.534
DQFEM solutions with cubic serendipity interpolation functions								
8	13.141	13.777	20.846	29.526	4.6379	6.7234	12.567	15.557
9	13.138	13.777	20.838	29.522	4.6372	6.7234	12.568	15.536
10	13.138	13.776	20.838	29.517	4.6372	6.7233	12.557	15.536
11	13.137	13.776	20.837	29.516	4.6372	6.7233	12.557	15.536
12	13.137	13.776	20.837	29.516	4.6372	6.7233	12.557	15.536
13	13.137	13.776	20.837	29.516	4.6372	6.7233	12.557	15.536

significant digits between the DQFEM results and the FEM results using T18 element citeg[56] are only two, but the same conclusion can also be found in Reference [56] when its method was compared with other methods.

In Table VI, the DQFEM solutions for six types of pentagonal plates agree with the *p*-version FEM solutions [55] and the standard FEM solutions by present authors, at least to three significant digits, and with the FEM solutions using T18 element [56] and the Fourier sine series solutions [90], to the first two significant digits. *FCCCC* means that the edge (1) is free, and all other edges are clamped, and so on.

Table III. The first four natural frequencies of clamped circular and elliptic plates ($\Omega = \omega a^2 \sqrt{\rho h / D}$).

					Mode sequences			
	1	2	3	4	1	2	3	4
$M = N$		$a/b = 1.0$				$a/b = 2.0$		
		Exact solutions [85]				*Rayleigh–Ritz solutions* [86]		
—	10.2158	21.26	34.88	39.771	27.3773	39.4976	55.9773	69.8557
	—					*Rayleigh–Ritz solutions* [87]		
—	—	—	—	—	27.377	39.497	55.985	69.858
DQFEM solutions with quartic serendipity interpolation functions								
9	10.2159	21.336	34.967	39.882	27.381	39.788	57.615	70.502
10	10.2161	21.261	34.875	40.268	27.379	39.529	56.490	69.873
11	10.2159	21.263	34.881	39.774	27.377	39.508	56.071	69.895
12	10.2159	21.261	34.876	39.797	27.377	39.500	55.998	69.856
13	10.2159	21.261	34.876	39.772	27.377	39.500	55.980	69.856
14	10.2159	21.261	34.876	39.772	27.377	39.499	55.978	69.855
15	10.2159	21.261	34.876	39.772	27.377	39.499	55.977	69.855
DQFEM solutions with cubic serendipity interpolation functions								
9	10.1999	21.304	34.983	39.828	27.310	39.775	57.677	70.277
10	10.2003	21.228	34.757	40.208	27.307	39.510	56.523	69.644
11	10.2001	21.230	34.778	39.713	27.305	39.488	56.099	69.663
12	10.2002	21.228	34.758	39.735	27.305	39.481	56.024	69.624
13	10.2002	21.228	34.759	39.710	27.305	39.480	56.006	69.624
14	10.2003	21.228	34.758	39.710	27.305	39.480	56.003	69.623
15	10.2002	21.228	34.759	39.710	27.305	39.480	56.003	69.623
DQM solutions with cubic serendipity interpolation functions [5]								
17	10.211	21.196	34.882	39.687	27.260	39.488	56.120	69.872
19	10.193	21.249	34.538	39.674	27.349	39.454	55.987	69.821
21	10.196	21.237	34.889	40.661	27.294	39.486	55.978	69.849
23	10.205	21.253	34.886	39.730	27.212	39.481	56.052	69.367
25	10.211	21.243	34.891	39.755	27.273	39.482	56.029	69.687

In Table VII, a comparison studies have been given for symmetric trapezoidal plates with four combinations of simply supported, clamped and free boundary conditions. *CFFF* indicates that the edge at $x = 0$ is clamped, and the like. The DQFEM solutions match with the DQM solutions [5, 66] and the Ritz solutions [63], at least to four significant digits. In Table VIII, the DQFEM solutions for clamped and simply supported rhombic plates with diagonal line ratio $a/b = 2.0$ and 3.0 are compared with the DQM solutions [5], the DSC solutions [72] and the superposition solutions [76]. One can obtain the same conclusions as above.

All in all, one can conclude that the DQFEM is capable of producing accurate and rapid convergent solutions for free vibration of thin plates with arbitrary shapes.

6. CONCLUSION

The present study is undertaken to develop a highly accurate and rapidly converging differential quadrature FEM and the corresponding curvilinear quadrilateral plate element by using DQ rules,

Gauss–Lobatto integration rule and variational principle. The DQFEM is essentially equivalent to the *p*-version FEM, while the DQFEM greatly simplifies the computations of the stiffness and mass matrices due to not using shape functions, and is capable of constructing curvilinear quadrilateral elements with any DOF and any order of inter-element compatibilities. The DQFEM precision is

Table IV. The first four natural frequencies of square plates ($\Omega_{ij} = \omega_{ij} a^2 \sqrt{\rho h / D}$).

	Mode shape							
	(1, 1)	(2, 1)	(1, 2)	(2, 2)	(1, 1)	(2, 1)	(1, 2)	(2, 2)
$M = N$	*CSCS* plate				*CCCC* plate			
	Kantorovich method [88]				*Kantorovich method* [88]			
	28.951	69.327	54.743	94.585	35.999	73.405	73.405	108.24
					Double trigonometric series [89]			
					35.985	72.394	72.394	108.22
DQFEM solutions with cubic serendipity interpolation function								
8	28.951	69.334	54.748	94.598	35.990	73.411	73.411	108.25
9	28.951	69.344	54.744	94.602	35.986	73.412	73.412	108.26
10	28.951	69.327	54.743	94.585	35.986	73.395	73.395	108.22
11	28.951	69.327	54.743	94.585	35.985	73.394	73.394	108.22
12	28.951	69.327	54.743	94.585	35.985	73.394	73.394	108.22
	FSFS plate				*FFFF* plate			
	Kantorovich method [88]				*Finite element analysis solutions*			
	9.631	16.135	38.945	46.738	13.466	19.597	24.274	34.796
DQFEM solutions with cubic serendipity interpolation function								
7	9.6314	16.135	39.113	46.897	13.469	19.596	24.270	34.805
8	9.6314	16.135	38.945	46.738	13.468	19.596	24.271	34.801
9	9.6314	16.135	38.946	46.739	13.468	19.596	24.270	34.801
10	9.6314	16.135	38.945	46.738	13.468	19.596	24.270	34.801
11	9.6314	16.135	38.945	46.738	13.468	19.596	24.270	34.801

Table V. The first four natural frequencies of triangular plates ($\Omega = \omega a^2 \sqrt{\rho h / D}$).

	Mode sequences							
	1	2	3	4	1	2	3	4
$M = N$	*CCC* plate ($d/a = b/a = 0.5$)				*SSS* plate ($d/a = b/a = 0.5$)			
The finite element method using T18 element [56]								
	186.80	311.64	389.82	474.54	98.66	197.12	256.11	333.49
The Rayleigh–Ritz method [62]								
	187.58	315.57	389.64	486.02	98.70	197.39	256.79	335.67
The differential quadrature finite element method								
10	187.50	317.10	390.16	487.02	98.54	197.34	256.58	335.32
12	187.54	316.23	389.79	486.19	98.62	197.37	256.59	335.45

Table V. *Continued*.

$M=N$	1	2	3	4	1	2	3	4
				Mode se	quences			
	CCC plate ($d/a=b/a=0.5$)				*SSS* plate ($d/a=b/a=0.5$)			
14	187.56	315.90	389.66	485.88	98.66	197.38	256.60	335.50
16	187.57	315.75	389.60	485.75	98.67	197.38	256.60	335.53
18	187.57	315.68	389.57	485.69	98.68	197.39	256.61	335.54
20	187.57	315.64	389.56	485.65	98.69	197.39	256.61	335.55
	CSS plate ($d/a=0, b/a=1$)				*SCC* plate ($d/a=0, b/a=1$)			
The modified superposition method [75]								
	65.790	121.08	154.45	196.38	73.394	131.58	165.00	210.52
The differential quadrature finite element method								
10	65.710	121.03	154.49	196.06	73.221	131.57	164.92	210.36
12	65.757	121.06	154.48	196.23	73.309	131.58	164.96	210.45
14	65.776	121.07	154.47	196.31	73.348	131.58	164.98	210.48
16	65.783	121.07	154.46	196.34	73.367	131.58	164.99	210.50
18	65.786	121.08	154.46	196.36	73.377	131.58	164.99	210.51
20	65.788	121.08	154.46	196.37	73.383	131.58	165.00	210.51
	FFF plate ($d/a=0, b/a=1$)				*Corner-supported* plate ($d/a=0, b/a=1$)			
The Rayleigh–Ritz method [57]								
	19.07	29.12	45.40	49.51	5.804	14.04	23.59	38.06
The differential quadrature finite element method								
10	19.057	29.118	45.359	49.474	5.8009	14.043	23.583	38.038
12	19.063	29.120	45.379	49.474	5.8024	14.043	23.588	38.050
14	19.065	29.122	45.387	49.475	5.8030	14.044	23.590	38.056
16	19.066	29.122	45.392	49.475	5.8033	14.044	23.591	38.058
18	19.067	29.122	45.394	49.475	5.8035	14.044	23.592	38.059
20	19.067	29.123	45.395	49.475	5.8036	14.044	23.592	38.060

Table VI. The first four natural frequencies of pentagonal plates ($\Omega=\omega(a^2/2\pi)\sqrt{\rho h/D}$).

$M=N$	1	2	3	4	1	2	3	4
				Mode se	quences			
	CCCCC plate				*SSSSS* plate			
10	3.1426	6.5035	6.5037	10.508	1.7434	4.4165	4.4182	7.8286
12	3.1461	6.5036	6.5038	10.511	1.7466	4.4192	4.4202	7.8356
14	3.1476	6.5037	6.5038	10.513	1.7481	4.4204	4.4210	7.8384
16	3.1483	6.5037	6.5038	10.513	1.7488	4.4210	4.4214	7.8397
18	3.1487	6.5037	6.5038	10.513	1.7492	4.4214	4.4217	7.8405
20	3.1489	6.5037	6.5038	10.514	1.7495	4.4216	4.4219	7.8409
*	3.1495	6.5054	6.5054	10.518	1.7492	4.4223	4.4223	7.8435
[55]	3.1493	6.5015	6.5015	10.512	—	—	—	—
[90]	3.1623	6.5395	6.5558	10.550	—	—	—	—

Table VI. *Continued.*

	Mode sequences							
	1	2	3	4	1	2	3	4
$M=N$	*CCCCC* plate				*SSSSS* plate			
[56]	3.1526	6.4419	6.5102	10.406	1.7490	4.4017	4.4070	7.7651
	FCCCC plate				*FSSSS* plate			
10	2.6697	4.0693	6.3812	7.0420	1.3747	2.8359	4.2696	5.6304
12	2.6686	4.0566	6.3806	7.0330	1.3760	2.8387	4.2715	5.6340
14	2.6684	4.0511	6.3804	7.0282	1.3766	2.8400	4.2724	5.6356
16	2.6684	4.0485	6.3804	7.0255	1.3770	2.8406	4.2728	5.6364
18	2.6685	4.0472	6.3805	7.0240	1.3771	2.8410	4.2731	5.6369
20	2.6686	4.0466	6.3805	7.0232	1.3773	2.8412	4.2733	5.6372
*	2.6690	4.0470	6.3821	7.0238	1.3772	2.8406	4.2743	5.6377
[56]	2.621	4.063	6.358	7.068	1.378	2.846	4.259	5.621
	FFFFF plate				*Corner-supported* plate			
10	1.5045	1.5052	2.4885	3.5604	0.8958	2.0804	2.0812	2.6884
12	1.5049	1.5052	2.4918	3.5605	0.8964	2.0807	2.0812	2.6888
14	1.5051	1.5052	2.4932	3.5605	0.8966	2.0809	2.0812	2.6889
16	1.5051	1.5052	2.4938	3.5605	0.8967	2.0810	2.0812	2.6891
18	1.5052	1.5052	2.4942	3.5605	0.8968	2.0811	2.0812	2.6891
20	1.5051	1.5052	2.4943	3.5604	0.8968	2.0812	2.0812	2.6891
*	1.5050	1.5050	2.4952	3.5608	0.8967	2.0801	2.0801	2.6891

*Calculated by present investigators using conventional FEM.

Table VII. The first four natural frequencies of symmetric trapezoidal plates ($\Omega=\omega(a^2/\pi^2)\sqrt{\rho h/D}$).

	Mode sequences							
	1	2	3	4	1	2	3	4
$M=N$	*CCCC* plate $(a/b=3.0, b/c=2.5)$				*SSSS* plate $(a/b=3.0, b/c=2.5)$			
10	10.428	15.568	21.484	23.908	5.3888	9.4180	14.662	15.908
12	10.427	15.563	21.476	23.906	5.3889	9.4208	14.676	15.908
14	10.427	15.563	21.476	23.905	5.3890	9.4216	14.679	15.908
16	10.427	15.563	21.476	23.905	5.3890	9.4219	14.681	15.908
[5]	10.427	15.563	21.476	23.905	5.3890	9.4219	14.680	15.908
[66]	10.427	15.563	21.476	23.905	5.3891	9.4223	14.682	15.908
	SCSC plate $(a/b=3.0, b/c=2.5)$				*CFFF* plate $(a/b=2, b/c=2)$			
10	9.4411	14.382	19.842	22.459	0.4237	1.4791	2.2957	4.2512
12	9.4427	14.385	19.883	22.470	0.4236	1.4788	2.2955	4.2503
14	9.4430	14.386	19.892	22.472	0.4236	1.4787	2.2954	4.2500
16	9.4431	14.386	19.895	22.472	0.4236	1.4787	2.2954	4.2499
[5]	9.4431	14.386	19.897	22.472	—	—	—	—
[63]	—	—	—	—	0.4236	1.4788	2.2955	4.2504

Table VIII. The first four natural frequencies of rhombic plates ($\Omega = \omega a^2 \sqrt{\rho h / D}$).

	Mode sequences							
	1	2	3	4	1	2	3	4
$M = N$	$a/b = 2.0$				$a/b = 3.0$			
SSSS plates								
10	5.6543	11.457	16.781	17.852	4.5810	8.1820	11.937	14.597
12	5.6602	11.457	16.810	17.857	4.5853	8.1813	11.935	14.624
14	5.6628	11.457	16.821	17.859	4.5857	8.1812	11.936	14.634
16	5.6643	11.457	16.826	17.860	4.5852	8.1812	11.936	14.637
18	5.6652	11.457	16.829	17.861	4.5845	8.1812	11.937	14.637
20	5.6658	11.457	16.831	17.861	4.5838	8.1812	11.936	14.637
DQM [5]	5.6776	11.457	16.854	17.865	4.6198	8.1812	11.947	14.707
DSC [72]	5.678	11.455	16.859	17.862	4.621	8.183	11.950	14.712
[76]	5.640	11.46	16.78	17.86	4.507	8.178	11.91	14.50
CCCC plates								
10	10.581	18.026	24.719	25.840	8.7940	13.504	18.345	21.758
12	10.579	18.026	24.697	25.822	8.7822	13.489	18.178	21.589
14	10.579	18.026	24.694	25.822	8.7788	13.489	18.173	21.562
16	10.579	18.026	24.694	25.821	8.7777	13.489	18.173	21.555
18	10.579	18.026	24.693	25.821	8.7773	13.489	18.172	21.552
20	10.578	18.026	24.693	25.821	8.7771	13.489	18.172	21.551
DQM [5]	10.578	18.026	24.693	25.821	8.7770	13.489	18.172	21.550
DSC [72]	10.580	18.036	24.697	25.823	8.776	13.489	18.173	21.557
[76]	10.58	18.03	24.69	25.82	8.774	13.49	18.18	21.56

validated through the eigenvalue problem analysis of freely vibrating plates with different types of regular and irregular planforms. The DQFEM solutions were found, in general, to be in excellent agreement with the exact and numerical solutions in literature.

The DQFEM can be directly applied to the static and dynamic analysis of beams, shells the in-plane and out-of-plane problems of plates and 3D problems. Malik and Civan's comprehensive comparison study [91] has shown that the DQM stands out in numerical accuracy as well as computational efficiency over FDM and FEM. DQFEM has overcome the limitations of the DQM pointed out by Bert and Malik [18], and is hoped to be a competitive method with FEM for analysis of large-scale problems.

NOTATION

$\mathbf{A}^{(r)}$, $\mathbf{B}^{(s)}$	weighting coefficient matrices of the partial derivatives
$\bar{\mathbf{A}}^{(r)}$, $\bar{\mathbf{B}}^{(s)}$	the assemblages of $\mathbf{A}^{(r)}$ and $\mathbf{B}^{(s)}$ according to $\bar{\mathbf{f}}$
$\tilde{\mathbf{A}}^{(r)}$, $\tilde{\mathbf{B}}^{(s)}$	weighting coefficient matrices of partial derivatives for curvilinear domain
$A_{ij}^{(r)}$, $B_{ij}^{(s)}$	elements of $\mathbf{A}^{(r)}$ and $\mathbf{B}^{(s)}$
$\bar{A}_{kp}^{(r)}$, $\bar{B}_{kp}^{(s)}$	elements of $\bar{\mathbf{A}}^{(r)}$ and $\bar{\mathbf{B}}^{(s)}$
a, b, c, d, e	dimensions of plates with different planforms
C_i^x, C_j^y	Gauss–Lobatto weights with respect to x and y directions, respectively

D	$D = Eh^3/12(1-\upsilon^2)$ is bending rigidity of plate
$\mathbf{E}$	diagonal unit matrix
E	Young's modulus
$\bar{\mathbf{F}}^{(r+s)}$	weighting coefficient matrix of mixed partial derivatives
$\bar{F}_{kp}^{(r+s)}$	elements of $\bar{\mathbf{F}}^{(r+s)}$
$\bar{\mathbf{f}}$	vector with elements f_{ij}
f_{ij}	function values of $f(x,y)$ at grid point (x_i, y_j)
h	thickness of plate
i, j, k, m, n	integers
$\mathbf{J}$	Jacobian matrix
$\mathbf{K}$	element stiffness matrix
l_j	Lagrange polynomials
$\mathbf{M}$	element mass matrix
M	the number of gird points in the x or ξ direction
N	the number of grid points in the y or η direction
N_{ij}	shape functions
$\mathbf{Q}$	transformation matrix from $\bar{\mathbf{w}}$ to $\mathbf{w}$
$\mathbf{q}$	distributed surface force vector
q	transverse distributed surface force
r, s	the order of partial derivatives with respect to x and y coordinates, respectively
$\mathbf{R}$	element load vector
S	the area of actual plate
S_k	serendipity interpolation functions defined in the natural $\xi - \eta$ plane
U	strain energy
W	work potential
$\mathbf{w}, \bar{\mathbf{w}}$	element displacement vectors
w	deflection of plate
w_{ij}	deflection at grid point (x_i, y_j)
x, y, z	Cartesian coordinates
ξ, η	natural Cartesian coordinates defined on the square parent domain
ρ	volume density
υ	the Poisson ratio
ω	angular frequency
Ω	dimensionless frequency

REFERENCES

1. Bellman R, Casti J. Differential quadrature and long term integration. *Journal of Mathematical Analysis and Applications* 1971; **34**:235–238.
2. Bellman R, Kashef BG, Casti J. Differential quadrature: a technique for the rapid solution of non-linear partial differential equations. *Journal of Computational Physics* 1972; **10**:40–52.

3. Civan F, Sliepcevich CM. Application of differential quadrature to transport processes. *Journal of Mathematical Analysis and Applications* 1983; **93**:206–221.
4. Bert CW, Jang SK, Striz AG. Two new approximate methods for analyzing free vibration of structural components. *AIAA Journal* 1988; **26**:612–618.
5. Bert CW, Malik M. The differential quadrature method for irregular domains and application to plate vibration. *International Journal of Mechanical Sciences* 1996; **38**:589–606.
6. Jang SK, Bert CW, Striz AG. Application of differential quadrature to static analysis of structural components. *International Journal for Numerical Methods in Engineering* 1989; **28**:561–577.
7. Bert CW, Malik M. Free vibration analysis of thin cylindrical shells by the differential quadrature method. *Journal of Pressure Vessel Technology* 1996; **118**:1–12.
8. Bert CW, Wang X, Striz AG. Differential quadrature for static and free vibration analysis of anisotropic plates. *International Journal of Solids and Structures* 1993; **30**(11):1737–1744.
9. Sherbourne AN, Pandey MD. Differential quadrature method in the buckling analysis of beams and composite plates. *Computers and Structures* 1991; **40**:903–913.
10. Liu FL, Liew KM. Static analysis of Reissner–Mindlin plates by differential quadrature element method. *ASME Journal of Applied Mechanics* 1998; **65**:705–710.
11. Wang X, Bert CW, Striz AG. Differential quadrature analysis of deflection, buckling, and free vibration of beams and rectangular plates. *Computers and Structures* 1993; **48**:473–479.
12. Wang X, Bert CW. A new approach in applying differential quadrature and free vibrational analysis of beams and plates. *Journal of Sound and Vibration* 1993; **162**:566–572.
13. Shu C. Generalized differential–integral quadrature and application to the simulation of incompressible viscons flows including parallel computation. *Ph.D. Thesis*, University of Glasgow, July 1991.
14. Shu C, Richards BE. Application of generalized differential quadrature to solve two-dimensional incompressible Navier–Stokes equations. *International Journal for Numerical Methods in Fluids* 1992; **15**:791–798.
15. Malik M, Bert CW. Differential quadrature solution for steady state incompressible and compressible lubrication problems. *ASME Journal of Tribology* 1994; **116**:296–302.
16. Quan JR, Chang CT. New insights in solving distributed system equations by the quadrature methods—I. Analysis. *Computers in Chemical Engineering* 1989; **13**:779–788.
17. Quan JR, Chang CT. New insights in solving distributed system equations by the quadrature methods—II. Numerical experiments. *Computers in Chemical Engineering* 1989; **13**:1017–1024.
18. Bert CW, Malik M. Differential quadrature method in computational mechanics: a review. *Applied Mechanics Reviews* 1996; **49**:1–28.
19. Bellomo N. Nonlinear models and problems in applied sciences from differential quadrature to generalized collocation methods. *Mathematical and Computer Modeling* 1997; **26**:13–34.
20. Civan F, Sliepcevich CM. Application of differential quadrature to solution of pool boiling in cavities. *Proceedings of the Oklahoma Academy of Science* 1985; **65**:73–78.
21. Striz AG, Chen W, Bert CW. Static analysis of structures by the quadrature element method (QEM). *International Journal of Solids and Structures* 1994; **31**:2807–2818.
22. Chen WL. A new approach for structure analysis: the quadrature element method. *Ph.D. Dissertation*, University of Oklahoma, 1994.
23. Malik M, Bert CW. Vibration analysis of plates with curvilinear quadrilateral planforms by DQM using blending functions. *Journal of Sound and Vibration* 2000; **230**:949–954.
24. Shu C, Chen W, Du H. Free vibration analysis of curvilinear quadrilateral plates by the differential quadrature method. *Journal of Computational Physics* 2000; **163**:452–466.
25. Civan F, Sliepcevich CM. On the solution of the Thomas–Fermi equation by differential quadrature. *Journal of Computational Physics* 1984; **56**:343–348.
26. Malik M. Differential quadrature element method in computational mechanics: new developments and applications. *Ph.D. Dissertation*, University of Oklahoma, 1994.
27. Malik M, Bert CW. Implementing multiple boundary conditions in the DQ solution of higher order PDE's: application to free vibration of plates. *International Journal for Numerical Methods in Engineering* 1996; **39**(7):1237–1258.
28. Fung TC. Imposition of boundary conditions by modifying the weighting coefficient matrices in the differential quadrature method. *International Journal for Numerical Methods in Engineering* 2003; **56**:405–432.
29. Karami G, Malekzadeh P. A new differential quadrature methodology for beam analysis and the associated differential quadrature element method. *Computer Methods in Applied Mechanics and Engineering* 2002; **191**:3509–3526.

30. Karami G, Malekzadeh P. Application of a new differential quadrature methodology for free vibration analysis of plates. *International Journal for Numerical Methods in Engineering* 2003; **56**:847–868.
31. Wang X, Liu F, Wang X, Gan L. New approaches in application of differential quadrature method to fourth-order differential equations. *Communications in Numerical Methods in Engineering* 2005; **21**:61–71.
32. Shu C, Du H. Implementation of clamped and simply supported boundary conditions in the GDQ free vibration analysis of plates. *International Journal of Solids and Structures* 1997; **34**(7):819–835.
33. Shu C, Du H. A generalized approach for implementing general boundary conditions in the GDQ free vibration analysis of plates. *International Journal of Solids and Structures* 1997; **34**(7):837–846.
34. Liew KM, Han JB, Xiao ZM, Du H. Differential quadrature method for Mindlin plates on Winkler foundations. *International Journal of Mechanical Sciences* 1996; **38**(4):405–421.
35. Han JB, Liew KM. Numerical differential quadrature method for Reissner–Mindlin plates on two-parameter foundations. *International Journal of Mechanical Sciences* 1997; **39**(9):977–989.
36. Han JB, Liew KM. Analysis of annular Reissner–Mindlin plates using differential quadrature method. *International Journal of Mechanical Sciences* 1998; **40**(7):651–661.
37. Shu C, Wang CM. Treatment of mixed and nonuniform boundary conditions in GDQ vibration analysis of rectangular plates. *Engineering Structures* 1999; **21**:125–134.
38. Wang XW, Gu HZ. Static analysis of frame structure by the differential quadrature element method. *International Journal for Numerical Methods in Engineering* 1997; **40**:759–772.
39. Chen WL, Striz AG, Bert CW. A new approach to the differential quadrature method for fourth-order equations. *International Journal for Numerical Methods in Engineering* 1997; **40**(11):1941–1956.
40. Wu TY, Liu GR. A differential quadrature as a numerical method to solve differential equations. *Computational Mechanics* 1999; **24**:197–205.
41. Wang X, Wang YL, Chen RB. Static and free vibrational analysis of rectangular plates by the differential quadrature element method. *Communications in Numerical Methods in Engineering* 1998; **14**:1133–1141.
42. Wu TY, Liu GR. The generalized differential quadrature rule for fourth-order differential equations. *International Journal for Numerical Methods in Engineering* 2001; **50**:1907–1929.
43. Wang X, Wang Y, Zhou Y. Application of a new differential quadrature element method to free vibrational analysis of beams and frame structures. *Journal of Sound and Vibration* 2004; **269**:1133–1141.
44. Wang Y, Wang X, Zhou Y. Static and free vibration analyses of rectangular plates by the new version of differential quadrature element method. *International Journal for Numerical Methods in Engineering* 2004; **59**:1207–1226.
45. Lu CF, Zhang ZC, Chen WQ. Free vibration of generally supported rectangular Kirchhoff plates: state-space-based differential quadrature method. *International Journal for Numerical Methods in Engineering* 2007; **70**:1430–1450.
46. Liu FL, Liew KM. Static analysis of Reissner–Mindlin plates by differential quadrature element method. *ASME Journal of Applied Mechanics* 1998; **65**:705–710.
47. Liu FL, Liew KM. Differential quadrature element method for static analysis of Reissner–Mindlin polar plates. *International Journal of Solids and Structures* 1999; **36**:5101–5123.
48. Chen CN. DQEM and DQFDM irregular elements for analyses of 2-D heat conduction in orthotropic media. *Applied Mathematical Modeling* 2004; **28**:617–638.
49. Chen CN. DQEM analysis of in-plane vibration of curved beam structures. *Advances in Engineering Software* 2005; **36**:412–424.
50. Striz AG, Chen W, Bert CW. Free vibration of high-accuracy plate elements by the quadrature element method. *Journal of Sound and Vibration* 1997; **202**:689–702.
51. Chen WL, Striz AG, Bert CW. High-accuracy plane stress and plate elements in the quadrature element method. *International Journal of Solids and Structures* 2000; **37**:627–647.
52. Soh AK, Cen S, Long YQ, Long ZF. A new twelve DOF quadrilateral element for analysis of thick and thin plates. *European Journal of Mechanics A*, *Solids* 2001; **20**:299–326.
53. Soh AK, Long ZF, Song C. Development of a new quadrilateral thin plate element using area coordinates. *Computer Methods in Applied Mechanics and Engineering* 2000; **190**:979–987.
54. Leung AYT, Zhu B. Transverse vibration of thick polygonal plates using analytically integrated trapezoidal Fourier p-element. *Computers and Structures* 2004; **82**:109–119.
55. Bin Z, Leunga YT. New *p*-version plate elements and applications in structural vibration analyses. *Chinese Journal of Computational Mechanics* 2008; **25**(4):447–453.
56. Gbazi SSA, Barki FA, Safwat HM. Free vibration analysis of penta, heptagonal shaped plates. *Computers and Structures* 1997; **62**(2):395–407.
57. Abrate S. Vibration of point supported triangular plates. *Computers and Structures* 1996; **58**(2):327–336.

58. Karunasena W, Kitipornchai S. Free vibration of shear-deformable general triangular plates. *Journal of Sound and Vibration* 1997; **199**(4):595–613.

59. Singh B, Hassan SM. Transverse vibration of triangular plate with abitrary thickness variation and various boundary conditions. *Journal of Sound and Vibration* 998; **214**(1):29–55.

60. Liew KM, Hung KC, Sum YK. Flexural vibration of polygonal plates: treatments of sharp re-entrant corners. *Journal of Sound and Vibration* 1995; **183**(2):221–238.

61. Singh B, Saxena V. Transverse vibration of triangular plates with variable thickness. *Journal of Sound and Vibration* 1996; **194**(4):471–496.

62. Kim CS, Dickinson SM. The free flexural vibration of isotropic and orthotropic general triangular shaped plates. *Journal of Sound and Vibration* 1992; **141**:383–403.

63. Liew KM, Lim CW, Lim MK. Transverse vibration of trapezoidal plates of variable thickness: unsymmetric trapezoids. *Journal of Sound and Vibration* 1994; **177**(4):479–501.

64. Zong HZ. Free vibration analysis of isosceles triangular Mindlin plates by the triangular differential quadrature method. *Journal of Sound and Vibration* 2000; **237**(4):697–708.

65. Shu C, Chen W, Du H. Free vibration analysis of curvilinear quadrilateral plates by the differential quadrature method. *Journal of Computational Physics* 2000; **163**:452–466.

66. Karami G, Malekzadeh P. An efficient differential quadrature methodology for free vibration analysis of arbitrary straight-sided quadrilateral thin plates. *Journal of Sound and Vibration* 2003; **263**:415–442.

67. Malekzadeha P, Karamib G. Polynomial and harmonic differential quadrature methods for free vibration of variable thickness thick skew plates. *Engineering Structures* 2005; **27**:1563–1574.

68. Liew KM, Han JB. A four-node differential quadrature method for straight-sided quadrilateral Reissner/Mindlin plates. *Communications in Numerical Methods in Engineering* 1997; **13**:73–81.

69. Civalek Ö. Application of differential quadrature (DQ) and harmonic differential quadrature (HDQ) for buckling analysis of thin isotropic plates and elastic columns. *Engineering Structures* 2004; **26**:171–186.

70. Wang XW, Wang YL. Free vibration analyses of thin sector plates by the new version of differential quadrature method. *Computer Methods in Applied Mechanics and Engineering* 2004; **193**:3957–3971.

71. Civalek Ö. A four-node discrete singular convolution for geometric transformation and its application to numerical solution of vibration problem of arbitrary straight-sided quadrilateral plates. *Applied Mathematical Modelling* 2007; DOI: 10.1016/j.apm.2007.11.003.

72. Civalek Ö. Discrete singular convolution methodology for free vibration and stability analyses of arbitrary straight-sided quadrilateral plates. *Communications in Numerical Methods in Engineering* 2008; **24**:1475–1495.

73. Civalek Ö. Free vibration and buckling analyses of composite plates with straight-sided quadrilateral domain based on DSC approach. *Finite Elements in Analysis and Design* 2007; **43**:1013–1022.

74. Saliba HT. Free vibration of simply supported general triangular thin plates: an accurate simplified solution. *Journal of Sound and Vibration* 996; **196**(1):45–57.

75. Saliba HT. Transverse free vibrations of right triangular thin plates with combinations of clamped and simply supported boundary conditions a highly accurate simplified solution. *Journal of Sound and Vibration* 1995; **183**(5):765–778.

76. Gorman DJ. Accurate free vibration analysis of rhombic plates with simply supported and fully clamped edge conditions. *Journal of Sound and Vibration* 1988; **125**(2):281–290.

77. Sakiyama T, Huang M. Free-vibration analysis of right triangular plates with variable thickness. *Journal of Sound and Vibration* 2000; **234**(5):841–858.

78. Zhou L, Zheng X. Vibration of skew plates by the MLS-Ritz method. *International Journal of Mechanical Sciences* 2008; DOI: 10.1016/j.ijmecsci. 2008.05.002.

79. Saadatpour MM, Azhari M, Bradford MA. Vibration analysis of simply supported plates of general shape with internal point and line supports using the Galerkin method. *Engineering Structures* 2000; **22**:1180–1188.

80. Ng CHW, Zhao YB, Wei GW. Comparison of discrete singular convolution and generalized differential quadrature for the vibration analysis of rectangular plates. *Computer Methods in Applied Mechanics and Engineering* 2004; **193**:2483–2506.

81. Xing YF, Liu B. New exact solutions for free vibrations of rectangular thin plates by symplectic dual method. *Acta Mechanica Sinica* 2009; **25**:265–270.

82. Xing YF, Liu B. New exact solutions for free vibrations of thin orthotropic rectangular plates. *Composite Structures* 2009; **89**:567–574.

83. Kim CS, Dickinson SM. On the free, transverse vibration of annular and circular, thin, sectorial plates subject to certain complicating effects. *Journal of Sound and Vibration* 1989; **134**:407–421.

84. Ramakrishnan R, Kunukkaserll VX. Free vibration of stiffened circular bridge decks. *Journal of Sound and Vibration* 1976; **44**:209–221.
85. Leissa AW. Vibration of Plates. *NASA SP-160*. U.S. Government Printing Office: Washington, DC, 1969.
86. Lam KY, Liew KM, Chow ST. Use of two-dimensional orthogonal polynomials for vibration analysis of circular and elliptical plates. *Journal of Sound and Vibration* 1992; **154**:261–269.
87. Singh B, Chakraverty S. On the use of orthogonal polynomials in the Rayleigh–Ritz method for the study of transverse vibration of elliptic plates. *Computers and Structures* 1992; **43**:439–443.
88. Sakata T, Takahashi K, Bhat RB. Natural frequencies of orthotropic rectangular plates obtained by iterative reduction of the partial differential equation. *Journal of Sound and Vibration* 1996; **189**:89–101.
89. Sakata T, Hosokawa K. Vibrations of clamped orthotropic rectangular plates. *Journal of Sound and Vibration* 1988; **125**(3):429–439.
90. Iire T, Yamada G, Narita Y. Free vibration of clamped polygonal plates. *Bulletin of the JSME* 1978; **21**:1696–1702.
91. Malik M, Civan F. A comparative study of differential quadrature and cubature methods vis-à-vis some conventional techniques in context of convection–diffusion–reaction problem. *Chemical Engineering Science* 1995; **50**:531–547.